Vortex Structures in Planetary Plasma Wakes

Vortex Structures in Planetary Plasma Wakes

By

H. Pérez-de-Tejada

Cambridge
Scholars
Publishing

Vortex Structures in Planetary Plasma Wakes

By H. Pérez-de-Tejada

This book first published 2023

Cambridge Scholars Publishing

Lady Stephenson Library, Newcastle upon Tyne, NE6 2PA, UK

British Library Cataloguing in Publication Data
A catalogue record for this book is available from the British Library

ISBN (10): 1-5275-0110-8
ISBN (13): 978-1-5275-0110-2

CONTENTS

ABSTRACT

Measurements conducted with the Pioneer-Venus Orbiter (PVO) and the Venus Express (VEX) spacecraft in orbit around Venus have led to the detection of vortex structures in that planet´s plasma wake. Such features have a scale size comparable to the Venus radius and show a ~ 3 min rotation period directed in the anticlockwise sense when viewed from the wake. They have been identified in the Venus near wake and show a gradual displacement in the direction transverse to the solar wind and also towards the southern hemisphere. As a whole, the vortex structures have the tendency to form a corkscrew flow that streams along the wake and whose thickness gradually decreases with the downstream distance from Venus. The corkscrew flow structures have the tendency to become thinner with distance downstream from Venus and, as a result, planetary ions that stream in that direction will be gradually accelerated by the transport of the kinetic momentum of vortex motion to that of particles that move in the direction of the wake. An interpretation of the expansion of the solar wind into the umbra is produced by the thermal expansion of the plasma into the wake combined with effects produced by the Coriolis and the Magnus force in that region and that are related to the rotation of the Venus ionosphere. The position of the vortex structures also varies along the solar cycle and becomes closer to Venus during solar cycle minimum conditions. A near pressure balance occurs between the kinetic pressure of the vortex structures and the magnetic field pressure that accumulates around them. Such correlation depicts the strong association that is present between the plasma and the magnetic field fluxes in the Venus wake. The description of plasma features obtained from measurements conducted with spacecraft that probed through the Venus plasma environment lead to the identification of structures present along the wake. Calculations show that an effective value for the mean free path for wave-particle interactions in the Venus ionosheath is $\geq$ 1000 km as derived from the transfer of fluid dynamic properties.

Hector Pérez-de-Tejada
Institute of Geophysics, UNAM, México

I

INTRODUCTION

From the different features that have been inferred from measurements conducted with the Pioneer Venus Orbiter (PVO) and the Venus Express (VEX) spacecraft in orbit around Venus there is evidence of the presence of vortex structures in the Venus wake that reveal processes similar to those that occur in fluid dynamics. In the early analysis of the PVO data it was first communicated that the velocity direction of plasma ions in the near Venus wake showed a gradual deflection away from the anti-solar direction in energy cycles measured in that region (Pérez-de-Tejada et al., 1982a; 2012a). That gradual change indicates a local deflection in the motion of particle fluxes thus suggesting that the plasma flow modifies its direction and even becomes oriented back to Venus from the wake. Suitable examples of those measurements are reproduced in **Figure 1.1** where the direction of motion of plasma fluxes in consecutive energy steps in different PVO orbits show a nearly 180º reversal when projected in cylindrical coordinates.

From the collection of plasma ion fluxes measured during the first season of observations of the PVO we refer in that figure to a set of plasma data in which the velocity vectors of the ion fluxes exhibit sudden changes in the direction of the particle motion. Data are presented in **Table I** and apply to PVO measurements conducted in orbits 80, 68, 65 and 66, which were conducted in the vicinity of the midnight plane during the first season of observation of that spacecraft along its nearly polar oriented trajectory. The measurements conducted in each energy cycle of those orbits correspond to values obtained near the outbound (southern hemisphere) crossing of the upper boundary of the ionosphere (ionopause) and represent the most intense ion fluxes that were observed during that cycle. Each reading in the first column describes the time (in UT) when an observation was made together with the number of the corresponding energy step and the volt per charge value (in parenthesis). The flux intensity (which leads to the intensity values given in the right-side column) and the latitudinal collector of the plasma instrument where it was received (marked by the number 3 or 4) are indicated in the second column.

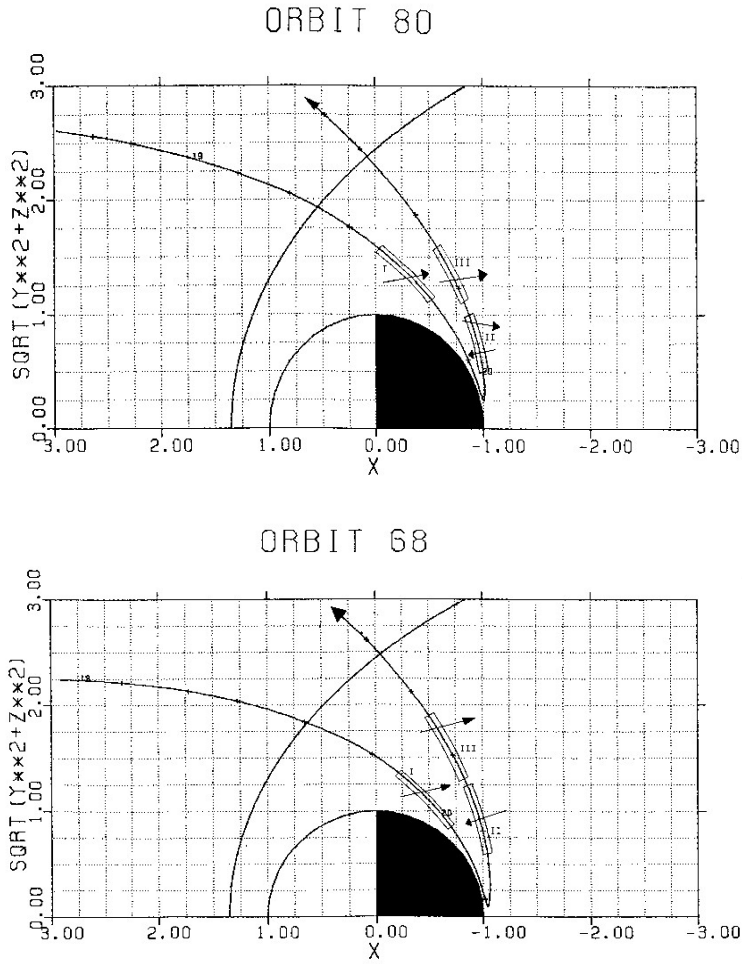

Fig. 1.1 Representative position of energy cycles (rectangular shapes) where measurements were made along the trajectory of the PVO in orbit 80 (upper panel) and in orbit 68 (lower panel) projected on a quadrant in cylindrical coordinates. As is indicated in Table I the arrows show schematically the (latitudinal) velocity direction of ion fluxes detected at different energy steps within each cycle of measurements. As shown in that Table sunward directed ion fluxes noted by an arrow across the rectangle labeled cycle II close to the planet is indicated in each figure (Pérez-de-Tejada, 1982a, 2012a).

Orbit 80 (19:59.16 UT)

energy step (V/q)		count	speed (km/s)		sector	α(°)	ions/cm² s sr
11 (257)	20:01.32 UT	107-4	236	59	119	-161	$3.7\ 10^7$
15 (495)	20:02.22 UT	101-4	308	77	109	-168	$3.2\ 10^7$
16 (583)	20:02.34 UT	101-3	336	84	101	-173	$3.2\ 10^7$
17 (686)	20:02.59 UT	95-4	360	90	367	14	$2.8\ 10^7$
18 (808)	20:03.11 UT	106-4	392	98	369	15	$3.6\ 10^7$
21 (1321)	20:03.48 UT	101-4	504	126	375	19	$3.5\ 10^7$

Orbit 68 (20:16.59 UT)

energy step (V/q)		count	speed (km/s)		sector	α(°)	ions/cm² s sr
1(50)	20:16.59 UT	102-3	96	24	438	65	$3.3\ 10^7$
2(59)	20:17.11 UT	104-4	104	26	430	58	$3.5\ 10^7$
4(82)	20:17.28 UT	107-4	124	31	192	-109	$3.7\ 10^7$
14(420)	20:19.53 UT	96-4	284	71	195	-107	$2.9\ 10^7$
15(495)	20:20.06 UT	97-4	308	77	190	-111	$2.9\ 10^7$
16(583)	20:20.18 UT	98-3	336	84	200	-104	$3.0\ 10^7$

Orbit 65 (20:16.39 UT)

energy step no. (V/q)		count	speed (km/s)		sector	α(°)	ions/cm² s sr
2(59)	20:16.51 UT	105-4	104	26	435	6	$3.5\ 10^7$
3(69)	20:17.04 UT	99-4	116	29	437	63	$3.1\ 10^7$
4(82)	20:17.16 UT	107-4	124	31	176	-120	$3.7\ 10^7$
10(218)	20:19.03 UT	101-4	208	52	185	-114	$3.2\ 10^7$
15(495)	20:19.45 UT	113-4	308	77	176	-120	$4.2\ 10^7$
18(808)	20:20.35 UT	98-4	392	98	439	65	$3.0\ 10^7$
21(1122)	20:21.12 UT	100-4	504	126	189	-111	$3.2\ 10^7$
25(2543)	20:22.14 UT	100-4	700	175	449	71	$3.2\ 10^7$
26(2996)	20:22.26 UT	100-4	732	183	195	- 107	$3.2\ 10^7$

Orbit 66 (20:19.25 UT)

energy step (V/q)		count	speed (km/s)		sector	α(°)	ions/cm² s sr
1(50)	20:19.25 UT	107-4	96	24	182	-11	$3.1\ 10^7$
9(185)	20:21.16 UT	116-4	188	47	449	71	$4.6\ 10^7$
11(257)	20:21.41 UT	102-4	220	55	200	-104	$3.3\ 10^7$
14(420)	20:22.18 UT	109-4	284	71	127	-155	$3.9\ 10^7$
17(656)	20:23.08 UT	117-4	364	91	456	76	$4.7\ 10^7$
24(2159)	20:24.35 UT	100-4	644	161	350	2	$3.2\ 10^7$

Table I. Ion flux intensity values (right side column) measured during an energy cycle in the outbound pass of the VO in orbits 80, 68, 65, and 66 through the Venus near wake (the energy steps in the left column for orbits 80 and 68 correspond to those in cycle II shown in Figure 1.1). The timing of the ion fluxes (in UT) is given in that column, together with the energy step number and its volts per charge value (in parenthesis). Their count number and the latitudinal collector of the plasma instrument where the fluxes were measured are shown in the second column (ion fluxes in collectors 3 and 4 are northbound directed implying that fluxes converge toward the plasma wake from the southern hemisphere). Their speed for H+ and O+ ions is indicated in the third and fourth columns. The azimuthal sector and the corresponding azimuthal angle α where the fluxes were detected are indicated in the fifth and sixth columns (sectors above or below ~347.5 correspond to positive or negative α values with sunward directed fluxes in the later cases), from Pérez-de-Tejada et al., 2012a.

Values of the calculated particle speed if they represent either H+ or O+ ions, together with the azimuthal sector (and the azimuthal angle α), are presented in the third through the sixth columns. The most notable example in the data for orbit 80 is shown in the upper panel of **Figure 1.1** where there are measurements with fluxes directed with a sunward component (negative α values). These are observed between the energy steps number 11 and 16 (first column in **Table 1**), and there are also ion fluxes measured along the solar wind direction (positive α values) between the energy steps number 17 and 21. Comparable variations are also present in the data set of the other orbits with a distribution of the azimuthal α angle that is persistent in orbit 68 (as in orbit 80), and then fluctuating orientations in orbits 65 and 66.

A schematic representation of the direction of the particle fluxes in orbit 80 is described in the upper panel of **Figure 1.1** for 3 different energy cycles of measurements together with the PVO trajectory projected on one quadrant using cylindrical coordinates (the outbound pass with cycles II and III occurs in the southern hemisphere but have been projected to the same quadrant). The position of the spacecraft during the energy cycle I initiated at 19:34.27 UT in the inbound pass, and the energy cycles II and III initiated at 19:59.16 UT and at 20:08.43 UT in the outbound pass are shown in that figure (each cycle is marked by a rectangular shape). The arrows indicate the latitudinal direction of arrival of the particle fluxes corresponding to the orientation of the collector of the plasma instrument where they were observed (measurements made in collector labeled 4 in **Table 1** during the outbound pass correspond to particle fluxes reaching the most northbound direction detected by the instrument ($22.5^o < \theta < 69^o$), and is opposite to those made in collector 1 which would be the most southbound directed collector of the instrument [Intriligator et al., 1989]. During the energy cycle I in the inbound pass and also in the energy cycle III in the outbound pass there is a tendency for the particle fluxes to be directed away from the wake, thus implying the observation of northbound fluxes in the northern hemisphere (collectors 3 and 4) and also the observation of southbound fluxes in the southern hemisphere (collectors 1 and 2). Different conditions can be identified in the energy cycle II measured in the vicinity of the outbound crossing of the ionopause that is reported in **Table 1**. In this cycle the (dominant) particle fluxes now converge toward the wake (all are detected in collectors 3 or 4) and exhibit directions either sunward directed (**negative α values**) or with an anti-sunward component (**positive α values**).

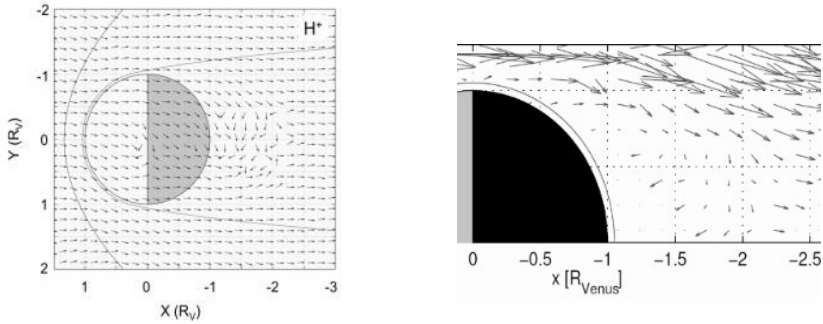

Figure 1.2. (left panel) Velocity vectors of the solar wind proton population projected on the ecliptic (XY) plane from measurements in VEX orbits across the Venus wake. A vortex structure is identified near the planet (Lundin et al., 2011). (right panel) Average direction of solar wind ion velocity vectors across the Venus near wake collected from VEX orbits and projected in cylindrical coordinates (Pérez-de-Tejada et al., 2017).

This later variation is indicated by large differences in the azimuthal sector number of the measurements which implies angles that may differ by up to 180º between both cases ($\alpha = 0$ corresponding to the antisolar direction). A similar distribution of velocity vectors in the Venus wake is observed in the data of orbit 68 of **Table 1** in energy cycles whose position along the PVO trajectory is reproduced in the lower panel of **Figure 1.1**. As it was the case for orbit 80 in the upper panel of that figure the northbound directed diverging particle fluxes are measured in the inbound pass (energy cycle I initiated at 19:53.22 UT), and southbound directed fluxes that also diverge from the wake are observed in the energy cycle III of the outbound pass initiated at 20:26.12 UT. In addition, particle fluxes measured in the inner ionosheath during cycle II in the outbound pass (initiated at 20:16.59 UT) and that were included in **Table I**, converge toward the wake and like those in orbit 80 also include velocity vectors with a sunward directed component (most notable flux intensities in the 4 to 16 energy steps) but there are also sporadic weak fluxes with an anti-sunward directed component in the lowest energies that were measured. The tendency in the data set of the outbound pass of orbits 80 and 68 is that the solar wind streaming near the ionopause (cycle labeled II) can acquire an orientation with a sunward directed component thus leading to a vortex structure (~180° change of the azimuthal α angle in that region).

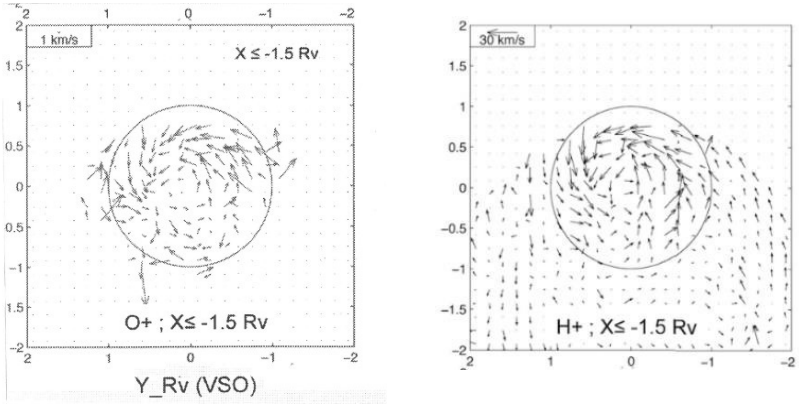

Figure 1.3. (right panel) Velocity vectors of the H+ ions projected on the YZ-plane compiled from the VEX measurements (≈ 1-300 eV). Notice the formation of a tail ward moving vortex (helix) in the near wake at X≤-1.5 R_V. (left panel) Velocity vectors of the O+ ions projected on the YZ-plane compiled from the VEX measurements. Notice the formation of a tail ward moving vortex (helix) in the near wake at X≤-1.5 RV (From Lundin et al., 2013).

Further and more extended information on this view was obtained from the VEX observations with indications of a vortex circulation pattern identified in the near wake region (Lundin et al., 2013: Pérez-de-Tejada et al., 2017). The left panel of **Figure 1.2** reproduces a velocity flow diagram projected on the XY (ecliptic) plane for the solar wind H+ ions measured across the wake. As it is the case in the PVO data in **Figure 1.1** there is evidence of a swirl motion in the near wake where the velocity vectors of the solar wind ions are even directed back to Venus. A similar pattern is obtained when they are plotted in cylindrical coordinates (right panel) with velocity vectors that become directed back to Venus in the central regions of the wake. A similar description was also inferred by Kollmann et al., (2016) from VEX measurements conducted far downstream along the wake. It is also notable that there is a velocity boundary layer across the wake with lower velocity values measured in its central region. A more extensive configuration for the swirl structure was also reported in **Figure 1.3** where the velocity vectors for the H+ (right panel) and for the planetary O+ ions (left panel) projected on the YZ plane perpendicular to the solar wind velocity direction define a vortex geometry. A general aspect of the swirl motion is that the rotation of the velocity vectors is in the counter clockwise sense when looked from the wake, and also that near the planet (at X< -1.5 R_V) they appear to occur across most of its cross-section. Also relevant is the fact that

the vortex motion has been found to apply separately to the ion and to the electron components and thus the particle components produce an electric current due to their different gyro-radius. Such consideration derives from measurements of the magnetic field components across the Venus wake (Durand-Manterola and Flandes, 2022).

An outline of results that have led to the identification of vortex structures in the Venus wake will be first incorporated to stress the importance of fluid dynamics to the interpretation of measurements conducted in that planet´s environment. An initial discussion on a plasma transition embedded in the ionosheath as the outer limit of a velocity boundary layer along the flanks of the Venus wake will be followed later by a description of plasma channels that extend downstream from the polar regions. These issues will further assess the origin of a corkscrew flow structure that is produced in the Venus wake and that describes the distribution of the ionospheric articles dragged by the solar wind.

II

PLASMA TRANSITION ALONG THE FLANKS OF THE VENUS WAKE

2.1 – Early Measurements

In the plasma and magnetic field measurements conducted during the transit of the Mariner 5 and the Venera spacecraft by the flanks of the Venus ionosheath (Bridge et al., 1967; Shefer et al., 1979; Vaisberg et al., 1976; Romanov et al., 1979) it was noted that in addition to a bow shock crossing upfront from the planet there is evidence of a different plasma transition located in the ionosheath downstream from that feature. That transition marks changes in the properties of the solar wind that apply by the flanks of that region. Such changes are different from those expected at the boundary of an induced magnetosphere where the magnetic field intensity increases as a result of the pileup of magnetic field fluxes (Bertucci et al., 2011). Repeated measurements of that transition within the ionosheath have also been reported from the Pioneer Venus (PVO), and the Venus Express (VEX) spacecraft with indications that there is a drastic change in the distribution function of the measured ion population at the time where it is detected (Pérez-de-Tejada et al., 1995a, 2013).

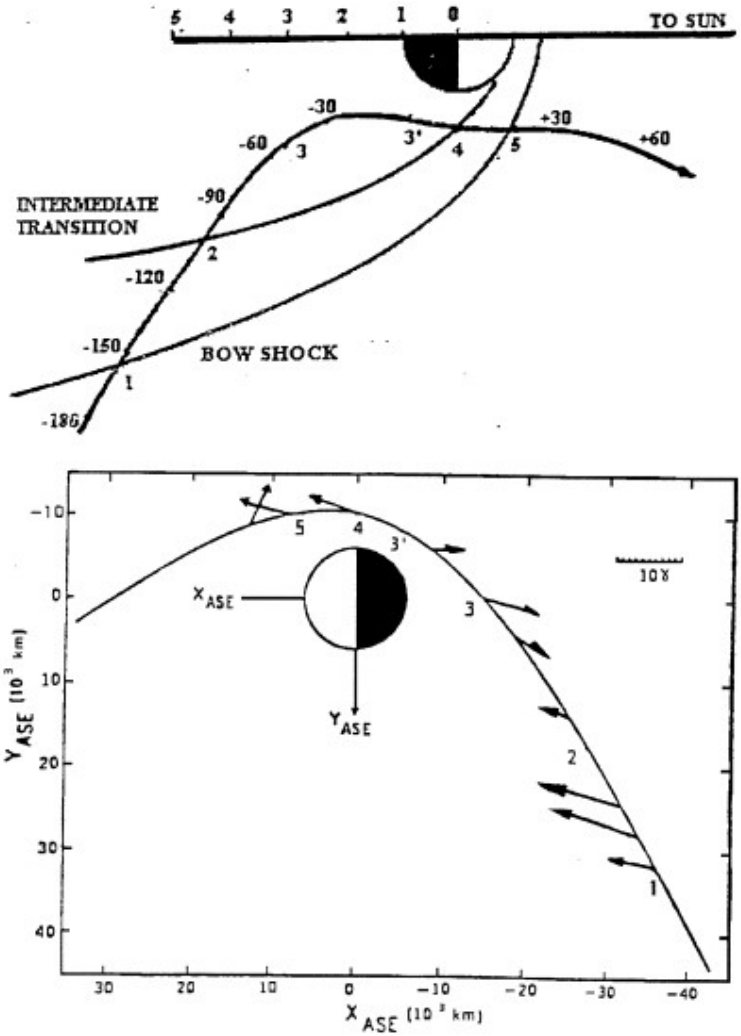

Figure 2.1. (upper panel) Trajectory of the Mariner 5 spacecraft projected in cylindrical coordinates in its flyby past Venus. The labels 1 through 5 along the trajectory mark important events in the plasma properties (bow shock, intermediate plasma transition). (lower panel) Trajectory of the spacecraft projected on the ecliptic plane to show a change in the polarity of the magnetic field direction behind the planet (Bridge et al., 1967).

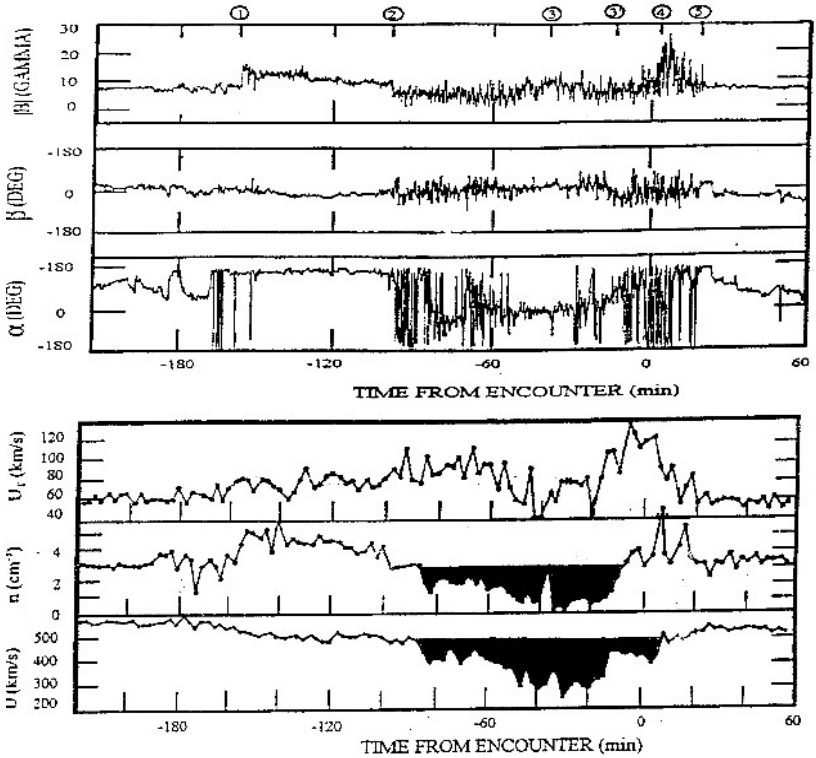

Figure 2.2. (upper panel) Magnetic field intensity and the latitudinal and azimuthal orientation of the magnetic field vector measured with the Mariner 5 spacecraft. (lower panel) Thermal speed, density, and bulk speed of the solar wind measured along its trajectory. (the shaded regions indicate the corresponding missing amounts of plasma density and bulk speed of the solar wind (from Bridge et al., 1967: Pérez-de-Tejada et al., 2000a).

An early indication of that feature is available from data obtained during the flyby of the Mariner 5 spacecraft by Venus with its trajectory being reproduced in cylindrical coordinates in the upper panel of **Figure 2.1** with features 1 through 5 marked on the trajectory (Bridge et al., 1967). A view of its transit projected on the ecliptic plane is presented in the lower panel of that figure to show the direction and the rotation of the magnetic field as the vehicle moved behind the planet. Values of the thermal speed, density, and bulk speed of the solar wind together with the magnetic field intensity and its latitudinal and azimuthal orientation are described in **Figure 2.2** to

indicate that strong oscillations of the magnetic field direction were measured as the spacecraft moved by its closest approach (Pérez-deTejada et al., 2000a). A transition different from the bow shock crossings which occurred at features 1 and 5 also marked at the top of that figure at 150 min before and 20 min after the encounter is seen to occur within the ionosheath at the locations labeled 2 and 4 at 90 min before and also at the encounter time. That transition marks the spacecraft transit through a feature that has been labeled the intermediate transition IT and that identifies a severe decrease of the flow speed and the density of the solar wind which is marked by the shaded region in both profiles of **Figure 2.2**. That variation implies the loss of the solar wind momentum that should have been employed to drive unrelated solar wind plasma along its direction of motion.

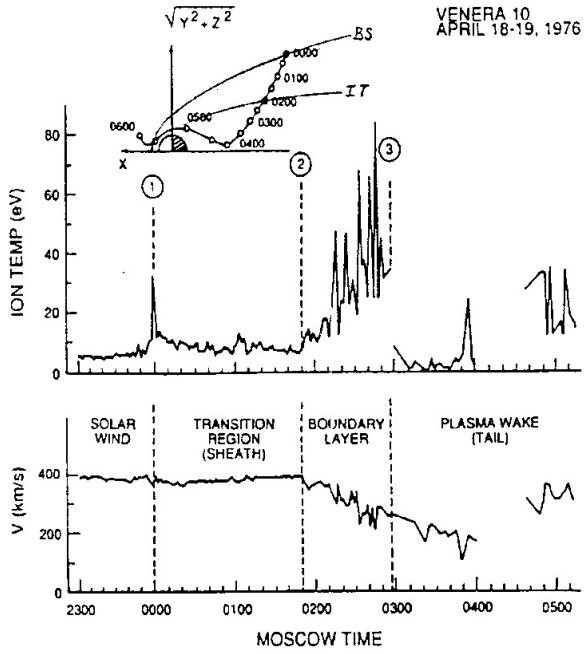

Figure 2.3. Ion speed and temperature measured along the orbit of Venera 10 on Apr. 19, 1976. The Venera orbit in cylindrical coordinates is shown at the top. The temperature burst at position 1 was recorded during a flank crossing of a bow shock. A boundary layer is apparent by the increase in temperature and decrease in speed and is initiated by the intermediate transition at position labeled 2. A latter discontinuity in the boundary layer temperature profile corresponds to the boundary of the magneto-tail. (from Romanov et al., 1979).

Evidence of the presence of that transition together with a sudden change in the plasma properties of the solar wind within the ionosheath are also available from an increase in the U_T thermal speed profile at feature 2 in **Figure 2.2**.This change together with an increase in the temperature and a decrease in the speed values were reported by Romanov et al., (1979) from the Venera data and are reproduced in **Figure 2.3** to show that in addition to a bow shock crossing by 00:00 MT there is a notable decrease of the flow speed with an accompanying increase of the plasma temperature through a sharp plasma transition by 01:50 MT.

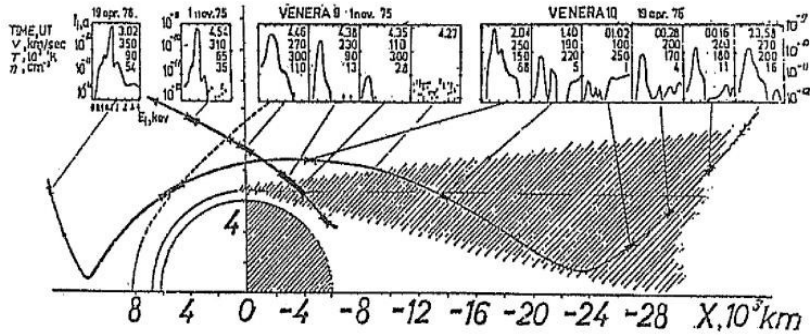

Figure 2.4. Representative ion spectra observed in the interaction region of Venus. Each data panel is connected by a line to a region in the trajectory where the data were obtained. The ordinate of each panel gives the ion current, and the abscissa the mean ion energy per charge. Figures inside each panel list (from top to bottom) time in UT, proton velocity in km/s, proton temperature, in multiples of 10^3 ºK, and number density per cm^3 (Verigin et al., 1978).

Both variations are further supported by measurements conducted with the wide-angle plasma analyzer onboard the Venera spacecraft where values of the speed, temperature and density of the H+ ions were obtained along its trajectory. These properties are reproduced in **Figure 2.4** as reported by Verigin et al., (1978) and indicate in separate panels for two different orbits that in addition to the bow shock crossing upfront from the planet there is evidence that the plasma temperature becomes larger by the transition region with values that reach ~ 250 10^3 ºK from lower ~ 90 10^3 ºK values that were measured outside that region. Such measurements are conducive to the observation of heated plasma within the interaction region between the solar wind and the Venus ionosphere measured by the flanks of the wake.

Further information on plasma heating in the inner ionosheath was also obtained from the PVO data where as shown in **Figure 2.5** the angular local temperature profiles in that region have a larger azimuthal width (labeled I) than that in the outer ionosheath labeled II (Pérez-de-Tejada., 1985).

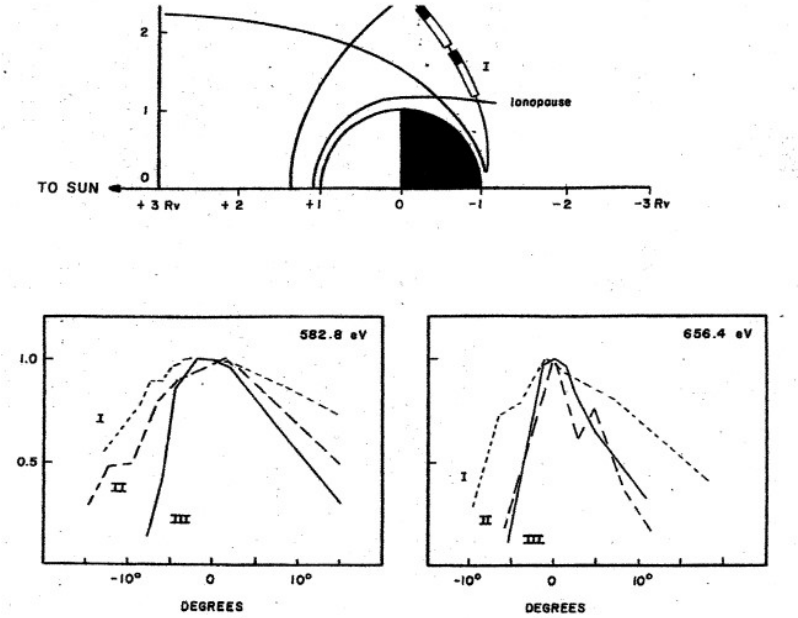

Figure 2.5. (upper panel) PVO trajectory during orbit 62 projected in cylindrical coordinates. Black boxes indicate the PVO position when angular scans were made in the inner and outer ionosheath (labeled I and II) together with measurements in the freestream solar wind (labeled III). (lower panel). The azimuthal distribution of peak particle fluxes measured in the 582.8 eV and 656.4 eV energy steps was obtained during three angular scans (Pérez-de-Tejada, 1985).

2.2 – PVO measurements

It has been found that the intermediate transition is mostly detected in the vicinity of the magnetic polar regions that occur where the piled up interplanetary magnetic field fluxes slip over the planet to enter the wake. A 3D view of such magnetic field lines distributed downstream from the planet is represented in the left panel of **Figure 2.6** to show how they hinge downstream from the planet behind a magnetic polar region. In that respect

the position of the intermediate transition (IT) is organized with respect to the global magnetic field orientation in the VSE coordinate frame around Venus and as shown in the right panel of **Figure 2.6** is seen to mostly occur in the vicinity of the magnetic polar regions (Pérez-de-Tejada, H., 1983). A general view of the plasma changes across the intermediate transition is summarized in **Figure 2.7** with a notable burst in the ion flux intensity measured in different orbits (upper panel), accompanied by a sudden change in the magnetic field intensity (middle panel), and a brief signal in the 30 kHz channel of the electric field detector of the PVO (lower panel). Such variations were detected in the data of PVO orbits that were mostly traced from the northern to the southern hemispheres near the midnight plane of the Venus wake (Pérez-de-Tejada et al., 1993a, 1995b).

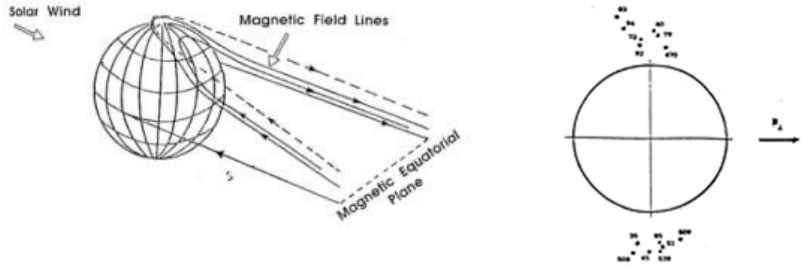

Figure 2.6. (left panel) 3D view of the magnetic field lines that have piled up around the Venus ionosphere and slide over the planet to enter the wake from the magnetic polar regions (Pérez-de-Tejada et al., 1983). (right panel) Position of the PVO spacecraft on the YZ plane in crossings of a plasma transition measured in the ionosheath. In each pass the PVO has been plotted with respect to the magnetic field direction rotated to the horizontal axis (inbound and outbound passes are shown in the top and bottom sides, Pérez-de-Tejada, 1983).

From the frequent observation of these features as the spacecraft moved across the wake in the vicinity of the midnight plane it was possible to select the data obtained in orbit 87 as representative of the various changes that the plasma flow exhibits in the ionosheath. These are shown in **Figure 2.8** where the PVO trajectory is projected on a quadrant traced in cylindrical coordinates in the upper panel to display the different ion flux intensity measured in consecutive energy scans of the plasma instrument in the outer and in the inner ionosheath.

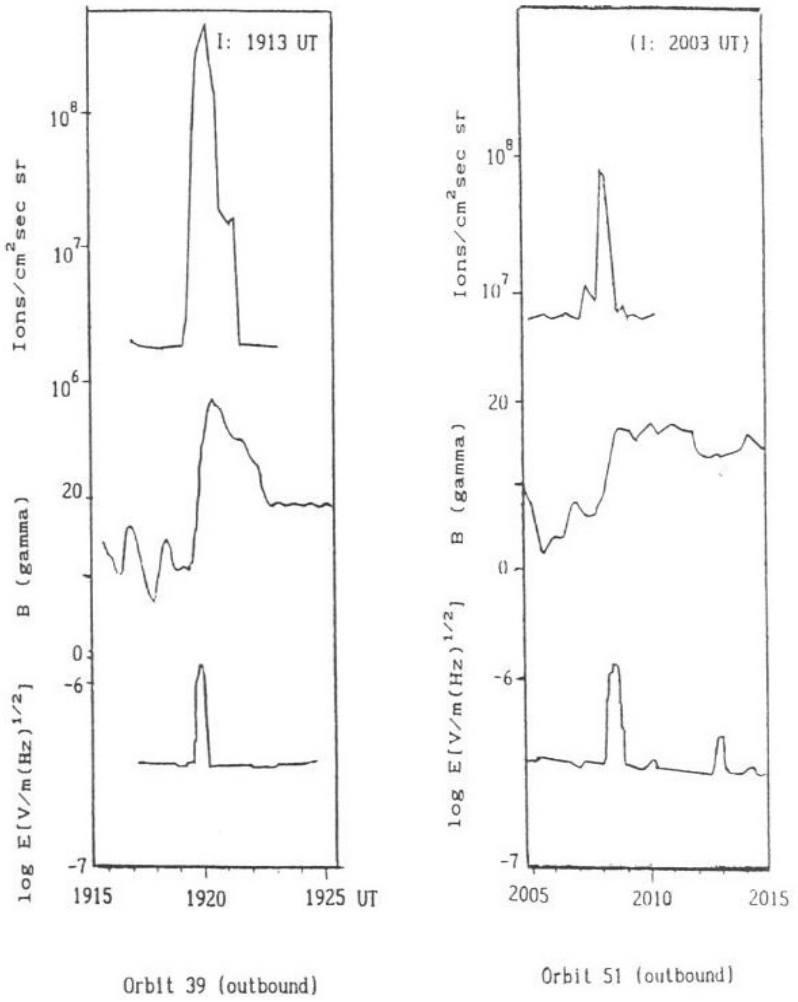

Figure 2.7. Ion flux intensity profile (upper panel), magnetic field intensity profile (middle panel), electric field profile with a burst in the 30 kHz channel (lower panel) measured in orbits 39 (left side) and 51 (right side). A plasma transition is identified by 1920 UT and by 2009 UT for each orbit (Pérez-de-Tejada et al., 1995).

In particular, the distribution function of those ion fluxes that are shown in the lower panel of **Figure 2.8** derive from measurements made inbound and outbound in the outer part of the ionosheath (labeled I and IV) and that have

similar ion flux intensities. A different ion flux distribution (labeled II) was measured in the inner ionosheath with smaller flux intensities situated at lower energy values and that may represent planetary ions (Intriligator, 1982). A more spectacular ion flux distribution was obtained in the energy cycle (labeled III) which depicts two different peak values located in a different energy range. Each of those peak values are comparable to those measured in the inner and in the outer ionosheath and thus imply a sharp change in the particle flux intensity as can be encountered across a plasma transition (Pérez-de-Tejada, et al., 1995b, 1996).

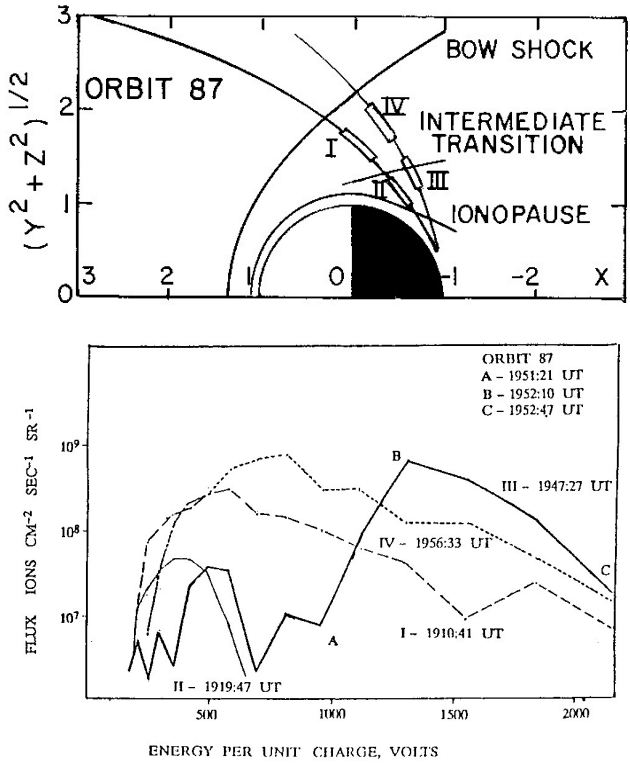

Figure 2.8. (upper panel) Trajectory of the PVO projected on one quadrant in cylindrical coordinates. The bow shock, the intermediate transition and the ionopause are indicated. (lower panel) Energy spectra of ions measured in the energy cycles I, II, III, and IV including their start time (their position is noted in the upper panel along the PVO trajectory). Positions A, B, and C in spectrum III mark the time when ion fluxes were calculated (from Pérez-de-Tejada et al., 1995b).

Arguments related to mass loading processes with a gradual change in the planetary ion composition that occurs in the solar wind at decreasing distance from the planet have also been addressed to produce that transition. However, such mechanism is not sufficient to describe the changes exhibited across that transition since it does not account for the enhanced plasma temperatures that are observed (Romanov et al., 1979: Verigin at al., 1978).

Issues related to effects that the intermediate transition and the velocity boundary layer in the ionosheath produce on the planetary ion population in the Venus upper ionosphere have also been examined in relation to the trans-terminator flow that was identified from the PVO observations (Knudsen et al., 1980). Measurements show that the upper dayside ionospheric plasma that drifts to the nightside can be accounted for from the deficit in the speed and density values measured outside in the inner ionosheath. **Figure 2.9** describes conditions related to the velocity vectors of that flow and that are mostly measured by the terminator (lower panel) with a profile of their speed values along the solar zenith angle (upper panel). It is notable that they reach 3-4 km/s by the terminator but they are not observed upfront from the ionosphere.

At the same time their intensity decreases sharply in the wake as it may be produced by turbulent motion of the flow in that region. It has been suggested that the trans-terminator flow may be produced by pressure gradient forces across the terminator (Knudsen et al., 1981) despite the fact that the flow speed values are supersonic and thus force conditions that are not present along that region; namely; a throat structure geometry as that shown in **Figure 8.1** would be necessary to make the flow reach supersonic values (Pérez-de-Tejada, 1986a, 1993b). A further constraint of the trans-terminator flow is that its effects are mostly measured by the midnight plane near and downstream from the magnetic polar regions while pressure gradient forces should be applicable all around the terminator plane.

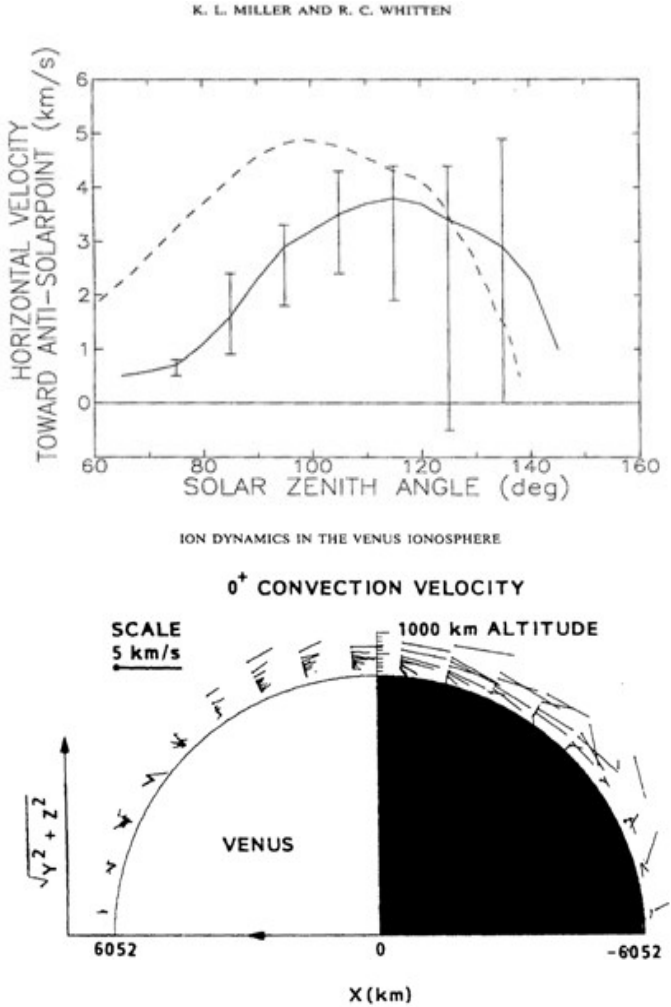

Figure 2.9. (lower panel) Vector velocity speeds of the trans-terminator flow in the Venus upper ionosphere measured with instruments onboard the Pioneer Venus Orbiter spacecraft (Knudsen et al., 1980). (upper panel) Approximate range of values of the trans-terminator flow speed measured in the Venus upper ionosphere as a function of the solid zenith angle (the peak speed values reach 3-4 km/s). (Miller and Whitten, 1982).

2.3 – Plateau density profiles in the Venus wake

Measurement of electron densities in the Venus wake obtained with the OETP instrument of the PVO revealed plasma clouds and ionospheric holes and that also show extended regions with substantial electron density values along the wake. Examples of those cases are presented in **Figure 2.10** to display electron density profiles that maintain values comparable to those of the nightside ionosphere up to high altitudes. In all three orbits there is a tendency for the electron density to exhibit nearly constant values from low (~ 150 km) altitudes to very high (~2000 km) distances. The profile in the right side (orbit 502) is peculiar because the plateau feature is interrupted by a region with very low densities between 10:55 UT and 11:00 UT and that resemble an ionospheric hole. The number of PVO orbits with density profiles like those in **Figure 2.10** is plotted as a function of the local solar time to show in **Figure 2.11** that they are mostly observed in the 02-22 hrs. LST range (Pérez-de-Tejada, 1995c). Most of those orbits occur in the vicinity of the midnight plane and were collected from the first and third seasons of PVO operation.

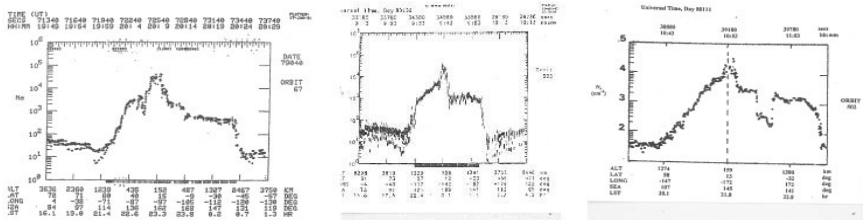

Figure 2.10. Electron density profiles in the Venus night side ionosphere measured in the PVO orbits 67, 523, and 502. In the last profile there is a density plateau at the sides of an ionospheric hole (Pérez-de-Tejada, 2005).

An association between the density plateau regions and ionospheric holes can be better distinguished in their identification at the local solar time where they are observed and that is indicated in **Figure 2.12** for several orbits. As a whole there is a tendency to occur in the vicinity of each other (Pérez-de-Tejada et al., 2005). A view based on effects related to the erosion of the local ionosphere and that is produced by the streaming plasma within the holes can be advanced to account for that agreement. These statements apply around the ionospheric holes by the central regions of the wake and are different from the assumption that the trans-terminator flow is produced by pressure gradient forces across the terminator which are applicable all

around the terminator. As shown in **Figure 2.10** the density distribution by the sides of that feature is indicative that ionospheric plasma is being dragged by the solar wind.

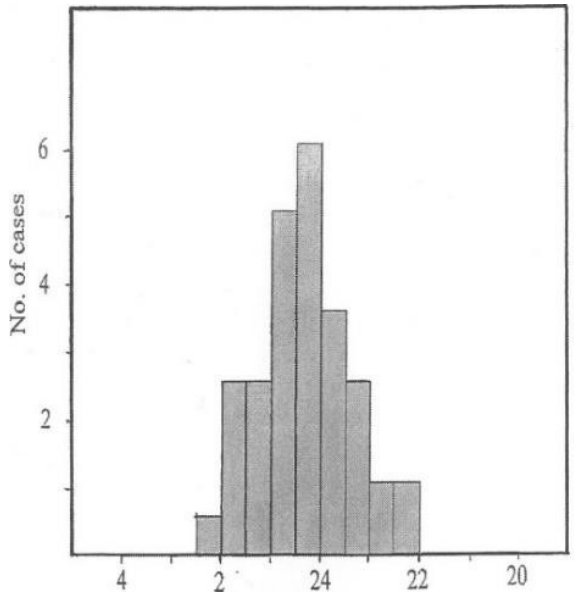

Figure 2.11. Histogram showing the distribution of cases when an electron density plateau is observed as a function of local solar time in PVO orbits selected from the first and the third seasons of operation (Pérez-de-Tejada, 2005).

2.4 – The intermediate transition in the PVO electric field data

The intermediate transition identified in the Mariner 5 and Venera plasma data was also revealed in the data of the PVO spacecraft from measurements in the 30 kHz channel of its electric field probe. A suitable example of those measurements is presented in **Figure 2.13** to show electric field profiles obtained across the ionosheath. Frequently, the 30 kHz channel measurements that exhibit variations associated with the observation of an electric burst in that channel imply a local sharp change in the local plasma density. Such signals correspond to plasma waves whose frequency is due to waves produced in the 8-15 cm^{-3} density range and reveal their presence when measuring variations of the local plasma density through that range.

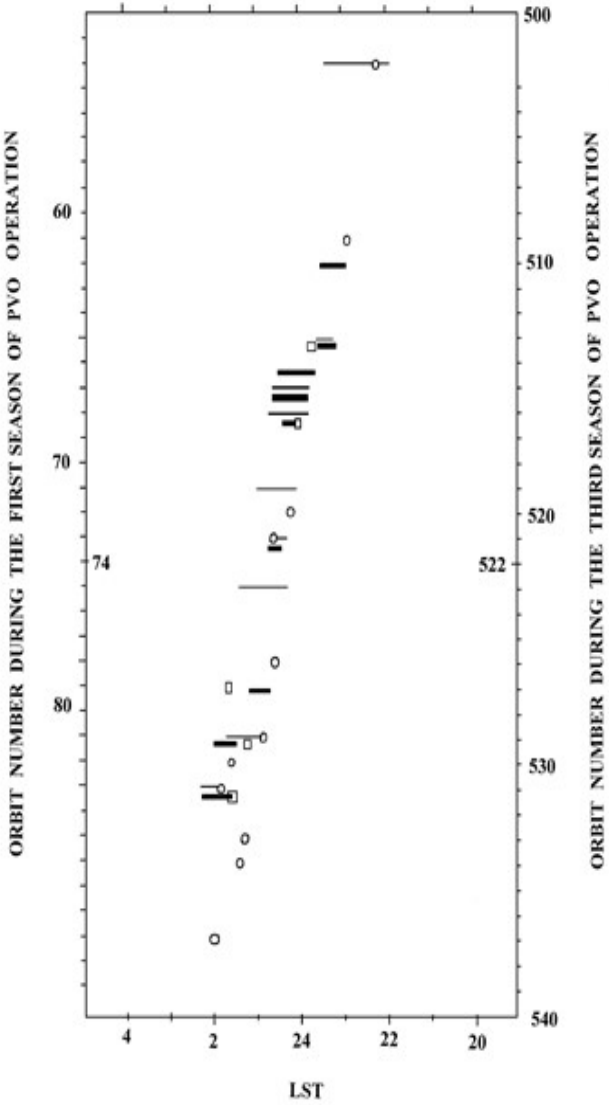

Figure 2.12. Comparative position in local solar time of ionosphere holes (circles) and extended ionospheric electron density profiles (lines) as those shown in Figure 2.10 that were detected in two seasons of PVO observations (Pérez-de-Tejada, 2005).

These conditions are employed to identify changes in the plasma density measured in the Venus ionosheath so that electric signals triggered at that frequency indicate sudden variations in the plasma density. Thus, the position of the spacecraft where the electric field bursts in the 30 kHz channel are observed identifies the location where a change in the plasma density event took place. In particular, after a bow shock crossing took place at 19:25 UT in the inbound pass of the PVO orbit 80 (middle panel in **Figure 2.13)** there is a plasma density change at a transition at 19:38 UT where an electric field burst in the 30 kHz channel was measured. That event occurred during the energy cycle labeled II in measurements made with the PVO plasma instrument indicated in the lower panel before the ionopause was later crossed at 19:45 UT. From such measurements it was possible to identify the position of that transition in other PVO orbits where there is also a notable change in the shape of the ion distribution. The sharp drop in the flux intensity in the ion distribution in the bottom panel of **Figure 2.13** occurred at the time when the burst in the 30 kHz channel of the electric field probe was measured.

The data in other PVO passes were examined to examine whether a similar correlation between both observations occurred at the same time and that is reproduced in **Figure 2.14.** A burst in the electric field profile in the 30kHz channel between the bow shock and the ionopause crossings also occurred in those cases. Data points corresponding to the position of the PVO in the inbound and outbound passes through the Venus ionosheath are presented in **Figure 2.15** in cylindrical coordinates (Pérez-de-Tejada et al., 1991a). While the burst in the 30 kHz channel occurred by and downstream from the terminator there is no indication in that plot about the preferable observation of the intermediate transition by the magnetic polar regions that was indicated in **Figure 2.6**. A similar variation is also apparent along the X-axis since they seem to be bow shock transition (Slavin et al., 1980). In addition, their Y- coordinate value is very small indicating that VEX probed near the midnight plane. As a whole both transitions have the tendency to be located closer to the planet along the Z-axis as solar minimum conditions approach by 2009. A similar variation is also apparent along the X-axis since they seem to be displaced at smaller distances from Venus under such conditions.

A comparative example with energy spectra of the VEX measurements that show both transitions will later be reproduced in **Figure 4.2** for the August 22/2006 orbit where the IT is detected inbound at 01:30 UT, and a BS transition is detected outbound at 02:50 UT. In both transitions there is a sudden change in the intensity of the energy spectra of the H+ ions (top